AIP | The Journal of Chemical Physics

A new smoothing function to introduce long-range electrostatic effects in QM/MM calculations

Dong Fang, Robert E. Duke, and G. Andrés Cisneros

Citation: The Journal of Chemical Physics **143**, 044103 (2015); doi: 10.1063/1.4926652
View online: http://dx.doi.org/10.1063/1.4926652
View Table of Contents: http://scitation.aip.org/content/aip/journal/jcp/143/4?ver=pdfcov
Published by the AIP Publishing

A new smoothing function to introduce long-range electrostatic effects in QM/MM calculations

Dong Fang,[1,2,a)] Robert E. Duke,[1,a)] and G. Andrés Cisneros[1,b)]
[1]*Department of Chemistry, Wayne State University, Detroit, Michigan 48202, USA*
[2]*Department of Chemistry, University of Wisconsin, Madison, Wisconsin 53706, USA*

(Received 1 June 2015; accepted 1 July 2015; published online 23 July 2015)

A new method to account for long range electrostatic contributions is proposed and implemented for quantum mechanics/molecular mechanics long range electrostatic correction (QM/MM-LREC) calculations. This method involves the use of the minimum image convention under periodic boundary conditions and a new smoothing function for energies and forces at the cutoff boundary for the Coulomb interactions. Compared to conventional QM/MM calculations without long-range electrostatic corrections, the new method effectively includes effects on the MM environment in the primary image from its replicas in the neighborhood. QM/MM-LREC offers three useful features including the avoidance of calculations in reciprocal space (k-space), with the concomitant avoidance of having to reproduce (analytically or approximately) the QM charge density in k-space, and the straightforward availability of analytical Hessians. The new method is tested and compared with results from smooth particle mesh Ewald (PME) for three systems including a box of neat water, a double proton transfer reaction, and the geometry optimization of the critical point structures for the rate limiting step of the DNA dealkylase AlkB. As with other smoothing or shifting functions, relatively large cutoffs are necessary to achieve comparable accuracy with PME. For the double-proton transfer reaction, the use of a 22 Å cutoff shows a close reaction energy profile and geometries of stationary structures with QM/MM-LREC compared to conventional QM/MM with no truncation. Geometry optimization of stationary structures for the hydrogen abstraction step by AlkB shows some differences between QM/MM-LREC and the conventional QM/MM. These differences underscore the necessity of the inclusion of the long-range electrostatic contribution. © *2015 AIP Publishing LLC.* [http://dx.doi.org/10.1063/1.4926652]

INTRODUCTION

The hybrid Quantum Mechanics (QM)/Molecular Mechanics (MM) method[1,2] has been a very useful tool in studying chemical reactions in large systems where it is not possible to use QM methods exclusively.[3–5] QM/MM calculations provide a convenient way to include non-negligible environmental effects for reactions in extended systems such as enzymes, solutions, zeolites, and heterogeneous catalysts. An important effect that is included in QM/MM calculations involves the Coulomb interaction between the reacting (QM) region and the environment (MM). However, several QM/MM implementations that use this so-called "electrostatic embedding" neglect the crucial role of long-range effects.[6]

Early on, long-range forces in classical chemical and biochemical simulations were accounted for by means of truncation schemes, where the Coulomb interactions are neglected after a certain distance (cutoff).[7,8] This is also true of QM/MM simulations, and is still a popular method of choice. However, simulations with truncation methods have been shown to result in artifacts in the resulting structure and/or dynamics of the system.[8–19]

Various switching and shifting functions have been proposed to remedy artifacts that arise from the truncation of the Coulomb interactions in classical simulations. The aim of these functions is to smoothly reduce the energies and forces between interacting particles when one of the particles is close to the boundary for the cutoff to neglect the Coulomb interactions (cutoff boundary). Several of the new cutoff schemes are based on work of Wolf *et al.*[20] These methods enforce charge neutrality by a neutralizing term since the truncation sphere inside the cutoff radius was found to be not electroneutral. Most cutoff methods seem to perform satisfactorily in the 20–30 Å range.

Methods to account for long-range electrostatic effects in QM/MM calculations have also been developed. In this case, the inclusion of long-range effects results in additional complications due to the presence of the continuous QM electronic density. In particular, one needs to take into account how the continuous QM charge density will be accounted for in the interaction with the classical system for the purpose of the long-range effects. To this end, a number of methods have been proposed to explicitly introduce long-range electrostatics in QM/MM calculations.

In boundary potential models, a subset of the atoms, including the QM and a region of the MM subsystems are represented explicitly. The remaining infinite bulk, which may

[a)]D. Fang and R. E. Duke contributed equally to this work.
[b)]Email: andres@chem.wayne.edu

include the remainder of the solute (e.g., protein, zeolite, and metal organic framework) is represented by an effective boundary potential. Several algorithms based on this method have been implemented including the local reaction field method for empirical valence bond/molecular mechanics (EVB/MM),[21,22] the generalized solvent boundary potential (GSBP),[23,24] the solvated macromolecule boundary potential (SMBP),[25,26] and a similar method based on the spherical solvent boundary potential (SSBP).[27]

A second family of approaches relies on periodic boundary methods. The initial implementation of Ewald sums for QM/MM was developed for semiempirical Hamiltonians.[28,29] Nam *et al.* developed an implementation of Ewald for QM/MM that explicitly takes all long-range contributions into account and uses Mulliken charges to represent the QM subsystem in reciprocal space.[30] This method was subsequently modified to calculate the MM and QM/MM coulomb interactions with the smooth particle Mesh Ewald (PME) method.[31] This method has been used to include long-range electrostatic effects in the explicit polarization (X-pol) potential.[32] A modification of this method has been proposed where the QM subsystem is represented by ChElPG instead of Mulliken charges.[33] A similar approach has been developed using Ladd sums in the framework of semiempirical QM models.[34] A linear-scaling method based on the electrostatic potential (GEEP)[35,36] and a modified Ewald lattice summation for the long-range QM/MM potential has been implemented for density functional theory (DFT) based QM/MM simulations.[35,36]

Another possibility involves the use of a cutoff in conjunction with shifting or switching functions similar to those used for classical simulations.[37] McCann and Acevedo recently proposed a method based on these schemes to account for long-range electrostatics in QM/MM simulations.[38–40] The use of the shifting function avoids the discontinuity in the energy and obviates the need to represent the infinite bulk.

In this contribution, we propose a scheme denoted as QM/MM Long-Range Electrostatic Correction (QM/MM-LREC). QM/MM-LREC includes long-range electrostatic effects by means of a novel switching/shifting function and the use of the minimum image convention to avoid box edge effects. Here, each particle i interacts with all particles j (with the inter-particle distance denoted by r_{ij}) within a certain cutoff R_{cut}. Assuming that particle i is in the primary unit cell, when the distance r_{ij} is smaller than half of the box length, particle j in the same image is used. On the other hand, when r_{ij} is larger than half of the box length, particle j in the neighboring image around the primary unit cell is considered. This convention only includes the first replicas around the primary unit, thus avoiding the need to approximate the QM charge density for reciprocal space and the reciprocal calculation altogether. In addition, analytical Hessians are available for QM/MM-LREC as finite images are used in the calculation. This last feature is particularly useful for the efficient optimization of critical points on the potential energy surface.[41]

The paper is organized as follows, in the section titled Theory and computational details, we introduce the new smoothing function and how it is incorporated into the QM/MM scheme. After that, we present results and discussions on three systems used to test this method and their comparison to results calculated with PME or no cutoff calculations. These systems include a water box, a double proton transfer between two aspartic acids, and the geometry optimization of the stationary structures for the hydrogen abstraction step of the dealkylation reaction of 1-methyl adenine catalyzed by AlkB.[42]

THEORY AND COMPUTATIONAL DETAILS

The total energy in a QM/MM system can be divided in three parts as shown in Equation (1),

$$E_{total} = E_{QM} + E_{QM/MM} + E_{MM}, \tag{1}$$

where E_{QM} is the electronic energy for the QM subsystem, $E_{QM/MM}$ is the interaction energy between the QM and the MM regions, and E_{MM} is the energy for the MM part. $E_{QM/MM}$ is comprised of three components, electrostatic, van der Waals, and bonded terms as shown in Equation (2),

$$E_{QM/MM} = E_{electrostatics}(QM/MM) + E_{vdw}(QM/MM) + E_{MM\text{-}bonded}(QM/MM). \tag{2}$$

In the additive QM/MM scheme employed herein,[43] the Coulomb interaction between the QM and MM regions is treated by the "electrostatic embedding" approach, as denoted in Equation (3). Here, the point charges from the MM atoms are introduced in the QM Hamiltonian to explicitly polarize the QM wavefunction

$$E_{QM} + E_{electrostatics}(QM/MM) = \langle \psi | \mathrm{H}_{eff} | \psi \rangle. \tag{3}$$

For the proposed switching and smoothing function, initially developed by one of us (RED), the Coulomb interaction $E(q_i,q_j,r_{ij})$, gradient $f(q_i,q_j,r_{ij})$, and Hessian $h(q_i,q_j,r_{ij})$ between point charge i and j are calculated by Equations (4)–(6), respectively,

$$E(q_i,q_j,r_{ij}) = \begin{Bmatrix} \frac{q_iq_j}{r_{ij}}\left(1-\left(\frac{2}{R_{cut}^3}(R_{cut}-r_{ij})^3+\frac{-3}{R_{cut}^2}(R_{cut}-r_{ij})^2+1\right)^2\right) & r_{ij}\le R_{cut} \\ 0 & r_{ij}>R_{cut} \end{Bmatrix}, \tag{4}$$

$$f(q_i,q_j,r_{ij}) = \begin{Bmatrix} -\frac{q_iq_j}{r_{ij}^2}\left(1-\left(\frac{2}{R_{cut}^3}(R_{cut}-r_{ij})^3+\frac{-3}{R_{cut}^2}(R_{cut}-r_{ij})^2+1\right)^3\right) & r_{ij}\le R_{cut} \\ 0 & r_{ij}>R_{cut} \end{Bmatrix}, \tag{5}$$

$$h(q_i,q_j,r_{ij}) = \begin{Bmatrix} \frac{df(q_i,q_j,r_{ij})}{dr_{ij}} & r_{ij}\le R_{cut} \\ 0 & r_{ij}>R_{cut} \end{Bmatrix}. \tag{6}$$

TABLE I. Percentage error for Coulomb energies between water molecules calculated and RMS Coulomb gradient given by LREC with respect to PME and the computation time (Intel Core-i7-920 processor @ 2.66G with 12 GB memory) for both methods at different cutoffs for the interactions are shown in Table I.

Cutoffs (Å)	Percentage error for Coulomb energy (LREC vs PME)	Percentage error for final RMS Coulomb gradient (LREC vs PME)	Computing time for LREC (s)	Computing time for PME (s)
8	1.07	1.07	4.632	5.435
9	−0.87	1.05	5.028	5.768
10	1.55	0.68	5.244	5.035
11	−0.03	0.57	5.443	5.04
12	0.41	0.51	5.645	5.038
13	0.78	0.4	5.44	5.039
14	0.72	0.35	5.645	5.041
15	0.41	0.34	5.439	5.037
16	0.53	0.29	5.446	5.24
17	0.27	0.25	5.641	5.035
18	0.65	0.23	5.639	5.037
19	−0.44	0.2	5.638	5.241
20	0.2	0.18	5.844	5.433
21	0.24	0.16	6.04	5.434
22	−0.03	0.15	6.239	5.437
23	0.3	0.14	6.246	5.639
24	0.27	0.12	6.442	5.637
25	0.14	0.12	6.639	5.836
26	0.74	0.01	6.839	6.037
27	0.2	0.01	7.043	6.238
28	0.36	0.01	7.24	6.435
29	0.4	0.03	7.643	6.432
30	0.56	0.03	7.844	6.84

The use of the switching function results in the need to perform several modifications to enable the proper treatment of the long-range cutoff boundary for the iterative QM/MM optimization scheme.[43] In particular the point charges, ρ(q,r), corresponding to the MM environment that are used for the effective Hamiltonian are modified as denoted in Equation (7),

$$\rho(q,r) = \begin{Bmatrix} q\left(1 - \left(\frac{2}{R_{cut}^3}(R_{cut}-r)^3 + \frac{-3}{R_{cut}^2}(R_{cut}-r)^2 + 1\right)^2\right) & r \le R_{cut} \\ 0 & r > R_{cut} \end{Bmatrix}, \tag{7}$$

where q are the charges as represented by the Amberff99 force field,[44] and r is the distance between the MM atom and the center of mass of the QM region. This results in effectively screened charges for the MM atoms that are close to the long-range Coulomb cutoff boundary with respect to the QM subsystem when calculating the Coulomb interactions between the QM and MM regions. In this way, the effective Hamiltonian in Equation (3) explicitly includes the screened charges. For the interactions between the MM atoms, Equations (4)–(6) are used for calculating Coulomb interactions, their gradients, and Hessians. Note that Equations (4) and (5) would be the corresponding expressions used for purely classical MD simulations.

The results from QM/MM-LREC are compared with the corresponding calculations with the original QM/MM implementation, which we denote hereafter as QM/MM-conventional. Here, all the MM atoms are treated explicitly without any replica of the system for the calculations of both the

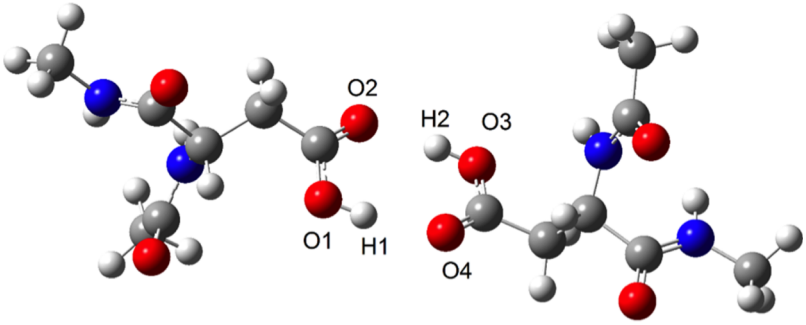

FIG. 1. Structure of the two aspartic acids (all waters are omitted for clarity).

TABLE II. The reaction coordinate R_H for the reactant and product, the relative energy of product with respect to the reactant (for each cutoff, the reactant is taken as zero), and the reaction barrier (the energy difference between TS and its corresponding reactant) at cutoffs 17 Å–30 Å by QM/MM-LREC.

Cutoff (Å)	R_H (reactant, Å)	R_H (product, Å)	Relative energy of product (kcal/mol)	Reaction barrier (kcal/mol)
17	−1.74	1.76	−5.0	18.1
18	−1.73	1.74	−2.7	19.2
19	−1.73	1.83	−5.0	16.9
20	−1.76	1.78	−2.8	18.5
21	−1.76	1.78	−2.5	18.7
22	−1.76	1.78	−2.9	18.5
23	−1.76	1.86	−4.1	18.4
24	−1.76	1.79	−3.2	18.4
25	−1.77	1.78	−2.8	18.4
26	−1.77	1.83	−4.3	18.3
27	−1.77	1.78	−3.0	18.4
28	−1.77	1.78	−3.2	18.4
29	−1.77	1.79	−3.2	18.4
30	−1.77	1.79	−3.3	18.6

QM/MM and MM Coulomb interactions. In this original implementation, the Coulomb interactions can also be damped with a polynomial function as implemented in TINKER[45] if a cutoff is specified.

All QM/MM calculations are handled by an in-house program that combines modified versions of Gaussian09[46] and TINKER.[45] During the MM optimizations, only atoms within 20 Å around the active site are allowed to move. For the calculations of the double proton transfer reaction, all atoms of the solute were treated as QM (50 QM atoms) and all solvent waters were represented by the MM environment. In the case of the geometry optimizations for the AlkB structures the system setup is described in detail in Ref. 42.

RESULTS AND DISCUSSION

The first system we studied is a water box with a size of 66 $Å^3$ to test LREC's performance in calculating the electrostatic energy using the smoothing function by classical MM only. As shown in Table I, the deviations for the Coulomb interaction and final RMS gradient calculated by LREC with respect to the corresponding results given by PME are 0.03%-1.55% and 0.01%-1.07%, respectively. At relatively small cutoffs, such as 8 Å-10 Å, the differences between LREC and PME are larger compared to values at the other cutoffs. For the absolute Coulomb energy, LREC gives the closest value to PME at 22 Å. For the final RMS gradient, the lowest value is around 26 Å-28 Å. Regarding the computation time, generally speaking, as expected for both LREC and PME methods, the computation time increases with the increase of the cutoff. Compared with PME, LREC requires larger computation time for the same cutoff, especially at relatively large cutoffs. However, since this method is easily parallelizable, it is expected that parallelization of this method will improve the performance with respect to Ewald-based methods, where the Fourier transform can become a bottleneck in parallel implementations, this will be explored in the future. The compromise between accuracy and computing time leads us to conclude that 22 Å provides the best accuracy vs. performance tradeoff.

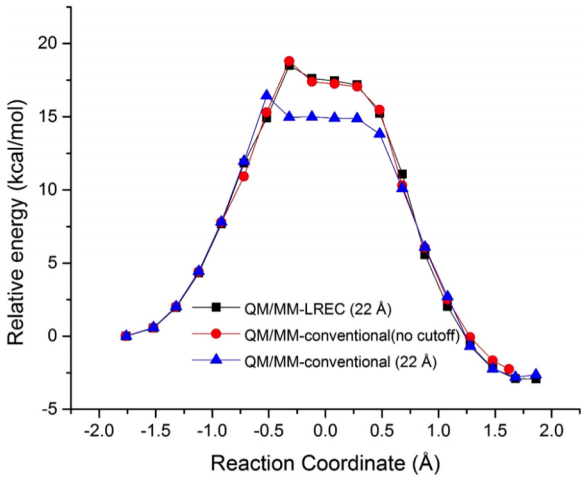

FIG. 2. The energy profile from the reaction coordinate driving method for QM/MM-LREC (cutoff = 22 Å) and QM/MM-conventional (no cutoff and cutoff = 22 Å).

The second test involves the reaction pathway optimization for the double proton transfer between two aspartic acids (see Figure 1 for the structure) with explicit water molecules by QM/MM-LREC. The reaction path has been optimized using the reaction coordinate driving method. The reaction coordinate (R_H) is defined as the linear combination

TABLE III. Several key distances (the numbering of the atoms in Figure 2) for the stationary structures calculated by QM/MM-LREC (cutoff = 22 Å) and QM/MM-conventional (no cutoff).

	QM/MM-LREC			QM/MM-conventional (no cutoff)		
Distance (Å)	Reactant	TS	Product	Reactant	TS	Product
d(O1-H1)	0.96	1.04	1.83	0.96	1.03	1.73
d(O4-H1)	1.84	1.42	0.95	1.85	1.44	0.96
d(O2-H2)	1.84	1.18	0.95	1.84	1.17	0.96
d(O3-H2)	0.96	1.22	1.94	0.96	1.23	1.82

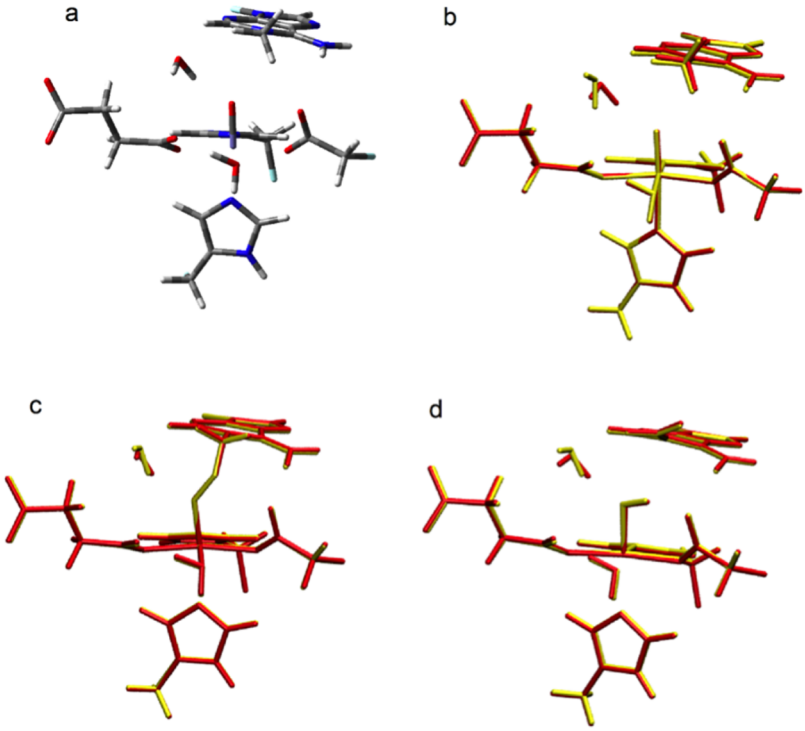

FIG. 3. (a) The structure of the reactant for the hydrogen abstraction by AlkB (red: oxygen; blue: nitrogen; white: hydrogen; gray: carbon; purple: iron; cyan: pseudo atoms), (b)–(d) overlaps of the reactant, TS, and intermediate (red: QM/MM-conventional; yellow: QM/MM-LREC).

TABLE IV. Decomposition of the total QM/MM energy E_{total} for the stationary structures by QM/MM-LREC and QM/MM-conventional (no cutoff).

	E_{QM} + $E_{electrostatic}$(QM/MM) (kcal/mol)		E_{vdw}(QM/MM) + $E_{MM\text{-}bonded}$(QM/MM) (kcal/mol)		E_{MM} (kcal/mol)	
Structure	QM/MM-LREC	QM/MM-conventional	QM/MM-LREC	QM/MM-conventional	QM/MM-LREC	QM/MM-conventional
Reactant	0	0	0	0	0	0
TS	23.0	23.1	0.2	−0.3	1.6	−0.4
Product	3.0	−0.4	−1.2	−0.6	−0.5	−2.7

of several key geometry parameters: $d_{O1\text{-}H1} + d_{H2\text{-}O3} - d_{O2\text{-}H2} - d_{O4\text{-}H1}$ (see Figure 1 for atom labels).

It can be observed from Table II that the energies along the reaction coordinate R_H for the reactant and product obtained when relatively small cutoffs are used (between 17 Å and 20 Å) show fluctuations. However, when the cutoff becomes larger than 20 Å, different cutoffs generate close reactant and product structures in most cases. Similarly, the energies for points on the reaction pathway are close to each other for different cutoffs above 20 Å most of the time. Cutoffs of 23 Å and 26 Å lead to a larger R_H for the product and lower relative energy.

Compared to the results from the QM-MM spherical scheme without any cutoff (QM/MM-conventional (no cutoff)), the relative energies along the pathways with cutoffs larger than 20 Å by QM/MM-LREC are close to those calculated by QM/MM-conventional (no cutoff). Additionally, the product is predicted to be around 2.3 kcal/mol lower than the reactant by QM/MM-conventional (no cutoff), and the approximate barrier is about 18.8 kcal/mol. These energies are consistent with the result given by QM/MM-LREC where the product is around 2-3 kcal/mol lower than the reactant and the corresponding energy barrier is around 18 kcal/mol for most of the cutoffs. Specifically, when the cutoff is 22 Å for QM/MM-LREC, the product is 2.9 kcal/mol lower than the reactant, and the reaction barrier is 18.5 kcal/mol.

TABLE V. Mülliken spin population for the QM/MM-LREC (QM/MM-conventional) optimized AlkB structures. Numbers in parentheses from Ref. 41.

	Reactant	TS	Intermediate
Fe	3.23(3.26)	4.21(4.24)	4.35(4.35)
O	0.58(0.54)	−0.19(−0.23)	0.27(0.26)
C	0.00(0.00)	−0.38(−0.38)	−0.92(−0.93)
H	0.00(0.00)	0.05(0.05)	0.01(0.01)

As shown in Figure 2, the comparison between the energy profile of the pathways by QM/MM-LREC with a cutoff of 22 Å and QM/MM-conventional (no cutoff) shows good agreement along the entire pathway. By contrast, when a cutoff of 22 Å is used for QM/MM-conventional, the barrier is noticeably underestimated. The comparison of several key distances (Table III) by QM/MM-LREC with QM/MM-conventional (no cutoff) shows that these two methods predict close reactant and transition state (TS) structures. However, two key distances for the product, d(O1-H1) and d(H2-O3),

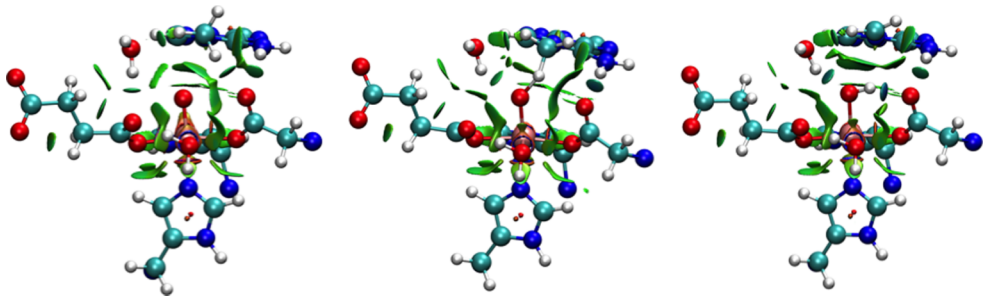

FIG. 4. NCI surfaces for the QM/MM-LREC optimized reactant (left), TS(middle), and product (right) AlkB structures. Gradient isovalue 0.5, $-0.05 < \rho\ \mathrm{sign}(\lambda 2) < 0.05$.

obtained with QM/MM-LREC are slightly longer than the ones from QM/MM-conventional (no cutoff). This indicates that the two aspartic acids are predicted to be more separated by QM/MM-LREC. In summary, for the reaction energy along the pathway for the double proton transfer between two aspartic acids, QM/MM-LREC with a cutoff of 22 Å gives close values to QM/MM-conventional (no cutoff).

The final test is the geometry optimization of the reactant, TS, and product structures (Figure 3(a) for the reactant) along the minimum energy pathway (MEP) for the hydrogen abstraction step of the dealkylation of 1-methyladine (1-meA) by AlkB using QM/MM-LREC.[42] The cutoff is chosen to be 22 Å, which performs well for both of the two tests above. The distances between the metal Fe and its surrounding ligands computed by QM/MM-LREC and QM/MM-conventional (cutoff = 15 Å) are close to each other (Figures 3(b)–3(d)). However, some deviation between these two schemes is observed for a H_2O molecule that forms a hydrogen bond to the oxo moiety bound to Fe. This water molecule is not directly coordinated to the iron but was previously shown to have a significant impact on the energetics of the system.[41] Because of this change in orientation, the calculated energies given by these two methods are different for these three stationary structures.

The calculated reaction barrier by QM/MM-LREC is 24.8 kcal/mol. This barrier is 2.4 kcal/mol higher than the one calculated by QM/MM-conventional of 22.4 kcal/mol. It is also noticeable that these two methods give different relative energies between the intermediate and the reactant. For QM/MM-conventional, the intermediate is 3.7 kcal/mol lower in energy than the reactant, while the intermediate is 1.3 kcal/mol higher in energy than the reactant for QM/MM-LREC. Similar to our previous study, the introduction of enthalpic and entropic effects (from the QM subsystem only as we previously showed the environment provides only a small de-stabilizing effect) results in a reduction of the barrier of approximately 3.5 kcal/mol. Our previous calculated free energy barrier of 18.6 kcal/mol is 1.2 kcal/mol lower than the estimated experimental barrier.[42] Using the energies obtained with QM/MM-LREC and the free energy correction, the calculated barrier is approximately 21.3 kcal/mol, giving almost the same error with respect to experiment (in the opposite direction) as our previous calculations.

The total QM/MM energy can be decomposed into three components, $E_{QM} + E_{electrostatic}(QM/MM)$, $E_{vdw}(QM/MM) + E_{MM\text{-}bonded}(QM/MM)$, and E_{MM}. The relative values of these three components for the TS and product with respect to the reactant are listed in Table IV. It can be seen from Table IV that the main contribution to the energy difference of the TS between these two methods is from E_{MM}, which is the total energy of the MM atoms. For the product, in addition to E_{MM}, the $E_{QM} + E_{electrostatic}(QM/MM)$ term also shows a large contribution to the energy difference between these two methods. These differences are due to the different treatments on each component by QM/MM-LREC and QM/MM-conventional. For $E_{QM} + E_{electrostatic}(QM/MM)$, fitted charges by Equation (7) within the cutoff are used, while QM/MM-conventional uses all the point charges that represent the MM atoms without any cutoff.

Interestingly, the calculated electronic properties between the corresponding structures are very similar. As shown in Table V, the Mülliken spin populations on selected atoms involved in the reaction are almost the same. Non-covalent interaction analysis with NCIPlot[47] shows almost all the surfaces for the corresponding structures are similar when compared with the previously reported surfaces (see Figure 4).[42] The only major difference observed is the water in the active site not coordinated to the Fe atom, which in the case of the QM/MM-LREC shows a blue surface between the O in this water and the succinate in the reactant. By contrast, this same water forms a hydrogen bond to the oxo in the QM/MM-conventional optimized reactant. The differences in the charge treatment and inclusion of the long-range Coulomb effects result in the change in orientation of the H_2O molecule which is not bound to the iron mentioned above, which in turn results in the energetic differences.

For the current QM/MM calculations, the evaluation of the QM region consumes much more computing time than the MM calculation in practice. Therefore, when it comes to the computing time, it is expected that the computing time for the calculations by QM/MM-LREC and QM/MM-conventional should be comparable.

CONCLUSIONS

We have presented an implementation of a new method to include long-range electrostatic effects for QM/MM calculations termed QM/MM-LREC. This scheme uses a new smoothing function under periodic boundary conditions (PBC) with the cutoff (half of the periodic box lengths). The use of the smoothing-switching function has several desirable traits

including the avoidance of reciprocal space calculations and thus having to reproduce (or approximate) the QM charge density in reciprocal space, and the availability of analytical Hessians. Our results show that at 22 Å cutoff, the new smoothing function exhibits close agreement in energy and gradient with PME (or no cutoff) results for the Coulomb interactions for a water box and for the prediction of the reaction pathway for the double proton transfer between two aspartic acids in a water box. The results for the hydrogen abstraction by AlkB from these two schemes show some differences. These differences may come from the usage of fitted charges that depend on the cutoff in QM optimization and different MM environment due to the MM optimization in QM/MM-LREC compared to QM/MM-conventional.

ACKNOWLEDGMENTS

The authors thank Wayne State's C&IT for computing time. This work was supported by the National Institutes of Health Grant No. R01GM108583.

[1]M. J. Field, P. A. Bash, and M. Karplus, J. Comput. Chem. **11**, 700 (1990).
[2]A. Warshel and M. Levitt, J. Mol. Biol. **103**, 227 (1976).
[3]H. M. Senn and W. Thiel, Angew. Chem., Int. Ed. **48**, 1198 (2009).
[4]M. W. van der Kamp and A. J. Mulholland, Biochemistry **52**, 2708 (2013).
[5]H. Hu and W. Yang, Annu. Rev. Phys. Chem. **59**, 573 (2008).
[6]G. A. Cisneros, M. Karttunen, P. Ren, and C. Sagui, Chem. Rev. **114**, 779 (2014).
[7]C. L. Brooks, B. M. Pettitt, and M. Karplus, J. Chem. Phys. **83**, 5897 (1985).
[8]P. J. Steinbach and B. R. Brooks, J. Comput. Chem. **15**, 667 (1994).
[9]P. Auffinger and E. Westhof, *Molecular Dynamics Simulations of Nucleic Acids* (John Wiley and Sons, New York, 1998).
[10]T. E. Cheatham III and P. A. Kollman, J. Am. Chem. Soc. **119**, 4805 (1997).
[11]H. E. Alper, D. Bassolino-Klimas, and T. R. Stouch, J. Chem. Phys. **99**, 5547 (1993).
[12]S. E. Feller, R. W. Pastor, A. Rojnuckarin, S. Bogusz, and B. R. Brooks, J. Phys. Chem. **100**, 17011 (1996).
[13]H. Schreiber and O. Steinhauser, Biochemistry **31**, 5856 (1992).
[14]D. M. York, W. Yang, H. Lee, T. A. Darden, and L. G. Pedersen, J. Am. Chem. Soc. **117**, 5001 (1995).
[15]J. D. Faraldo-Gomez, G. R. Smith, and M. S. P. Sansom, Eur. Biophys. J. **31**, 217 (2002).
[16]D. P. Tieleman, B. Hess, and M. S. P. Sansom, Biophys. J. **83**, 2393 (2002).
[17]M. Patra, M. T. Hyvönen, E. Falck, M. Sabouri-Ghomi, I. Vattulainen, and M. Karttunen, Comput. Phys. Commun. **176**, 14 (2007).
[18]M. Patra, M. Karttunen, M. T. Hyvönen, E. Falck, P. Lindqvist, and I. Vattulainen, Biophys. J. **84**, 3636 (2003).
[19]M. Patra, M. Karttunen, M. T. Hyvönen, E. Falck, and I. Vattulainen, J. Phys. Chem. B **108**, 4485 (2004).
[20]D. Wolf, P. Keblinski, S. Phillpot, and J. Eggebrecht, J. Chem. Phys. **110**, 8254 (1999).
[21]R. G. Alden, W. W. Parson, Z. T. Chu, and A. Warshel, J. Am. Chem. Soc. **117**, 12284 (1995).
[22]A. Warshel and A. Papazyan, Curr. Opin. Struct. Biol. **8**, 211 (1998).
[23]W. Im, S. Bernèche, and B. T. Roux, J. Chem. Phys. **114**, 2924 (2001).
[24]P. Schaefer, D. Riccardi, and Q. Cui, J. Chem. Phys. **123**, 014905 (2005).
[25]T. Benighaus and W. Thiel, J. Chem. Theory Comput. **5**, 3114 (2009).
[26]T. Benighaus and W. Thiel, J. Chem. Theory Comput. **7**, 238 (2011).
[27]A. Aleksandrov and M. Field, Phys. Chem. Chem. Phys. **13**, 10503 (2011).
[28]J. Gao and C. Alhambra, J. Chem. Phys. **107**, 1212 (1997).
[29]J. Gao, J. Phys. Chem. **96**, 6432 (1992).
[30]K. Nam, J. Gao, and D. M. York, J. Chem. Theory Comput. **1**, 2 (2005).
[31]R. C. Walker, M. F. Crowley, and D. A. Case, J. Comput. Chem. **29**, 1019 (2008).
[32]P. Zhang, D. G. Truhlar, and J. Gao, Phys. Chem. Chem. Phys. **14**, 7821 (2012).
[33]Z. C. Holden, R. M. Richard, and J. M. Herbert, J. Chem. Phys. **139**, 244108 (2013).
[34]F. Dehez, M. T. C. Martins-Costa, D. Rinaldi, and C. Millot, J. Chem. Phys. **122**, 234503 (2005).
[35]T. Laino, F. Mohamed, A. Laio, and M. Parrinello, J. Chem. Theory Comput. **1**, 1176 (2005).
[36]T. Laino, F. Mohamed, A. Laio, and M. Parrinello, J. Chem. Theory Comput. **2**, 1370 (2006).
[37]C. J. Fennell and J. D. Gezelter, J. Chem. Phys. **124**, 234104 (2006).
[38]O. Acevedo, J. Phys. Chem. A **118**, 11653 (2014).
[39]O. Acevedo and W. L. Jorgensen, Wiley Interdiscip. Rev.: Comput. Mol. Sci. **4**, 422 (2014).
[40]B. McCann and O. Acevedo, J. Chem. Theory Comput. **9**, 944 (2013).
[41]H. B. Schlegel, Wiley Interdiscip. Rev.: Comput. Mol. Sci. **1**, 790 (2011).
[42]D. Fang, R. L. Lord, and G. A. Cisneros, J. Phys. Chem. B **117**, 6410 (2013).
[43]Y. Zhang, H. Liu, and W. Yang, J. Chem. Phys. **112**, 3483 (2000).
[44]W. D. Cornell, P. Cieplak, C. I. Bayly, I. R. Gould, K. M. Merz, D. M. Ferguson, D. C. Spellmeyer, T. Fox, J. W. Caldwell, and P. A. Kollman, J. Am. Chem. Soc. **117**, 5179 (1995).
[45]J. W. Ponder, Washington University, Saint Louis, MO, 2008.
[46]M. J. Frisch, G. W. Trucks, H. B. Schlegel, G. E. Scuseria, M. A. Robb, J. R. Cheeseman, G. Scalmani, V. Barone, B. Mennucci, G. A. Petersson, H. Nakatsuji, M. Caricato, X. Li, H. P. Hratchian, A. F. Izmaylov, J. Bloino, G. Zheng, J. L. Sonnenberg, M. Hada, M. Ehara, K. Toyota, R. Fukuda, J. Hasegawa, M. Ishida, T. Nakajima, Y. Honda, O. Kitao, H. Nakai, T. Vreven, J. A. Montgomery, J. E. Peralta, F. Ogliaro, M. Bearpark, J. J. Heyd, E. Brothers, K. N. Kudin, V. N. Staroverov, R. Kobayashi, J. Normand, K. Raghavachari, A. Rendell, J. C. Burant, S. S. Iyengar, J. Tomasi, M. Cossi, N. Rega, J. M. Millam, M. Klene, J. E. Knox, J. B. Cross, V. Bakken, C. Adamo, J. Jaramillo, R. Gomperts, R. E. Stratmann, O. Yazyev, A. J. Austin, R. Cammi, C. Pomelli, J. W. Ochterski, R. L. Martin, K. Morokuma, V. G. Zakrzewski, G. A. Voth, P. Salvador, J. J. Dannenberg, S. Dapprich, A. D. Daniels, Ö Farkas, J. B. Foresman, J. V. Ortiz, J. Cioslowski, and D. J. Fox, GAUSSIAN 09, Gaussian, Inc., Wallingford, CT, 2009.
[47]J. Contreras-García, E. R. Johnson, S. Keinan, R. Chaudret, J.-P. Piquemal, D. N. Beratan, and W. Yang, J. Chem. Theory Comput. **7**, 625 (2011).